Int. J. Electrochem. Sci., 15 **(2020)** 4712 – 4721, doi: 10.20964/2020.05.85

International Journal of
ELECTROCHEMICAL
SCIENCE
www.electrochemsci.org

Titanium Dioxide Nanoparticle and Carbon Nanotube Incorporated Carbon Nanofiber Nanocomposite Modified Electrode for Hemoglobin Electrochemistry

Lin Zhu[1,3], *Yuhua Wang*[2], *Zhen Ai*[3], *Xi Zhang*[1], *Xiaoyan Li*[1], *Xiaoping Zhang*[1,*],*Wei Sun*[1,*]

[1] Key Laboratory of Water Pollution Treatment and Resource Reuse of Hainan Province, College of Chemistry and Chemical Engineering, Hainan Normal University, Haikou 571158, P. R. China
[2] Shandong Vocational Animal Science and Veterinary College, 261061, Weifang, P. R. China
[3] Key State Laboratory of Industrial Vent Gas Reuse, The Southwest Research & Design Institute of the Chemical Industry, Chengdu 610225, P. R. China
[*]E-mail: swyy26@hotmail.com

Received: 13 Janaury 2020 / *Accepted:* 3 March 2020 / *Published:* 10 April 2020

This study aimed to achieve direct electron transfer of bovine hemoglobin (Hb) on titanium dioxide nanoparticle and carbon nanotubes incorporated carbon nanofiber (TiO_2-CNT-CNF) nanocomposite modified carbon ionic liquid electrode (CILE). Electrochemical method was used to check the properties of the modified electrode (Nafion/Hb/TiO_2-CNT-CNF/CILE), which confirmed the realization of direct electrochemical reaction with a pair of well-shaped redox peaks on cyclic voltammograms. UV-visible and FT-IR spectra were used to prove the biocompatibility between nanocomposite and Hb molecules. The study also revealed that Nafion/Hb/TiO_2-CNT-CNF/CILE had well electrocatalytic reduction ability to trichloroacetic acid and hydrogen peroxide with good linear relationship between peak current and concentration. Quality analysis of medical sample solution was realized with satisfactory results. The paper demonstrated the potential application of TiO_2-CNT-CNF nanocomposite in the field of third generation electrochemical Hb sensor.

Keywords: Hemoglobin, Direct electrochemistry, Titanium dioxide, Carbon nanofiber, Carbon nanotube

1. INTRODUCTION

Unlike some traditional biochemical analysis that often use auxiliary chemical reagent, chromogenic agent with tedious separation and detection process, electrochemical biosensors show the properties including simple pretreatment, no additional reagent need, separation and detection completed simultaneously, and conversion of chemical signals into electrical signals for digit processing, which has always been an active research area in recent years. In this field, heme proteins

based modified electrodes have been widely reported with the challenges of promoting and addressing the multi-needs, such as enhanced sensitivity, lower detection limit, and testing of complex actual samples. Generally speaking, the deeply presence of redox-active center and unfavorable orientation of biomacromolecular protein on electrode are not benefit for electron transfer. Various modifiers or electrocatalysts such as polymers [1], metal oxides [2,3], metal nanoparticles[4,5], biomaterials[6], carbon materials[7] and composite materials[8-11] are used to increase the direct electron transfer rate of proteins on electrode interface. At the same time, some immobilization methods of protein are designed to enhance stabilization of the modified electrode with good tolerance.

Carbon materials are economically available substances with widely sources and stable chemical properties. Advanced carbon materials such as graphite [12], diamond [13], carbon nanotubes [14] and carbon foam [15] etc. are usual components of functional electrode materials for electrochemical applications. For example, Selvakumar et al. used graphene and β-cyclodextrin (β-CD) nanocomposite for immobilization of hemoglobin (Hb) to realize direct electrochemistry [16]. Sun et al. systematically reported direct electrochemistry of redox proteins at various carbon nanomaterials modified electrode with good electrocatalytic ability [17-20]. These studies prove that carbon nanomaterials with faster conductivity, larger surface area and better biocompatibility are benefit for the development of electrochemical sensors. Carbon materials can be divided into various classifications including three-dimensional structure nanodiamond, two-dimensional graphite, one-dimensional carbon nanotubes and quasi-zero-dimensional buck minster fullerene C_{60} [19]. Carbon nanofiber (CNF) is one of a one-dimensional (1D) carbon nanomaterial ranging from 10 to 500 nm in diameter and from 0.5 to 100 μm in length [20]. CNF has good electrical conductive and excellent structural properties, such as surface defects, exposed active groups, irregularity microarchitecture and favorable for surface reaction, which also allows better immobilization with other nanomaterial and biomolecules. Yang et al. prepared CNF/MnO_2 composites as high-capacitance supercapacitors with high specific capacitance and good rate capability [21]. Meng et al. prepared a functionalized S carrier for superior Li–S batteries composed by Co_9S_8/CNF complex [22]. Wang et al. synthesized CoS_2-CNFs by electrospinning and hydrothermal process to study electrochemical capacitance [23]. Niu et al. described the outstanding performances of CNFs and its related composite, which could provide optional materials in practical-oriented and high-quality biosensors [24].

In this article, TiO_2 nanoparticles and CNT incorporated CNF composite were synthesized by electrospinning and carbonization technology, which was used for electrode modification. Direct electron transfer of Hb modified electrode was investigated in detail. Results of electrochemistry and spectroscopy revealed that Hb showed fast electron transfer activity and maintained biological stability. By using this Hb modified electrode, quantitative analysis of trace trichloroacetic acid (TCA) and H_2O_2 in solution were realized, and further designed for the detection of medical samples.

2. EXPERIMENTAL METHODS

2.1. Chemicals

Bovine Hb (MW 64,500, Sigma), polyacrylonitrile (PAN, J&K Scientific Co., China). TiO_2 nanoparticles (Nanjing Xianfeng Nanotechnology Co., China, purity>99%, particle size 20~40 nm),

CNTs (purity>95%, main range of diameter<10 nm, length of 5~15 μm, Shenzhen Nanoport. Co., China), 1-hexylpyridinium hexafluorophosphate ($HPPF_6$, Lanzhou Yulu Fine Chem. Co., China), 30% H_2O_2 (Xilong Scientific Co., China) and TCA (Tianjin Kemiou Chem. Co., China) were used as received. The supporting electrolyte was 0.1 mol·L^{-1} phosphate buffer solutions (PBS). Double distilled water was used throughout the experiments. Unless otherwise specified, all other chemical reagents were used of analytical grade.

2.2. Preparation of TiO_2-CNT-CNF nanocomposite

TiO_2-CNT-CNF nanocomposites were prepared by electrospinning and thermal carbonization with the following procedure. Firstly, 1.683 g PAN powder, 0.450 g CNTs and 0.510 g TiO_2 NPs were added to 20 mL DMF with ultra-sonication for 20 minutes to obtain a well-dispersed TiO_2-CNT-PAN precursor solution. Secondly, based on the reference [20] electrospinning was carried using the following settings: spinning voltage (6 kV), liquid inlet flow rate (25 μL min^{-1}), the distance from the needle to the receiver (12 cm), and the cylinder receiver rotated at speed (1340 rpm). The resulted TiO_2-CNT-PAN nanofiber was heated with heating rate (5℃ min^{-1}) and carbonized at 800℃ for 2 hours in a tubular furnace (KMTF-1100, Anhui Kemi Machinery Technology, China) under N_2 atmosphere to get TiO_2-CNF-CNT nanocomposite.

2.3. Preparation of Nafion/Hb/TiO_2-CNT-CNF/CILE

CILE was fabricated by using a dry-mixture method with graphite powder:$HPPF_6$ mixture (mass ratio of 2:1) and glass electrode tube (Φ = 4 mm), which was used as the substrate electrode with its surface polished to mirror-like [25]. 5.0 μL of ultrasonically dispersed 1.0 mg mL^{-1} TiO_2-CNT-CNF aqueous suspension was coated on the surface of CILE to obtain TiO_2-CNT-CNF/CILE. After drying, 5.0 μL of 15 mg mL^{-1} Hb aqueous solution was applied on TiO_2-CNT-CNF/CILE surface to obtain the Hb/TiO_2-CNT-CNF/CILE. Finally, 6.0 μL of 0.5% Nafion solution was used to form stable film with the working electrode (Nafion/Hb/TiO_2-CNT-CNF/CILE) got, which was stored at 4℃ when not used.

2.4. Apparats

A CHI 1210A electrochemical workstation (Shanghai Chenhua Instrument, China) was applied in the electrochemical experiment with a N_2 deoxygenized electrolyte. Nafion/Hb/TiO_2-CNT-CNF/CILE was used as the working electrode with Ag/AgCl (3.0 mol·L^{-1} KCl) and platinum electrode served as the reference and the auxiliary electrode, respectively.

Nicolet 6700 Fourier transform infrared spectrometer (Thermo-Fisher Scientific Co., USA) and TU-1901 double-beam UV-vis spectrophotometer (Beijing General Instrument Ltd. Co., China) were used for spectroscopic investigations. Scanning electron microscopy (SEM) was performed a JSM-7100F scanning electron microscope (JEOL, Japan).

3. RESULTS AND DISCUSSION

3.1. Surface characterization of TiO_2-CNT-CNF nanocomposite

Electrospinning is a simple and versatile method for generating fiber polymer, which can be carbonized at high temperature to form CNF with excellent chemical stability and good electrical conductivity. The morphology of TiO_2-CNT-CNF nanocomposite on CILE was recorded by SEM at various magnifications (Fig. 1). The composite exhibited a typical and uniform line appearance with network formed by CNF. The enlarged image (Fig. 1D) showed evidently that TiO_2 NPs and CNT were distributed in outer and inner CNF, proving the evenly distribution of nanomaterials on the surface and inside of CNF. The SEM results proved that TiO_2-CNT-CNF was prepared with the formation of uniform nanostructures with controllable process.

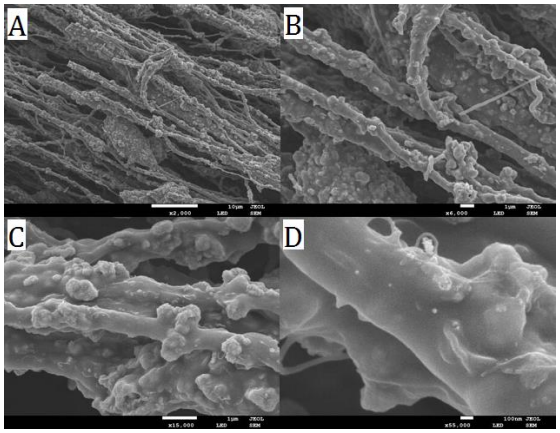

Figure 1. SEM image of TiO_2-CNT-CNF nanocomposite at different magnifications (A to D).

3.2. Spectroscopic analysis

The structural information of Hb was studied by FT-IR and UV-Vis spectrophotometry with the curves shown as Figure 2. In UV-visible spectra, the changes of the typical Hb Soret absorption band can provide information of Hb denaturation. In Fig.2A both the characteristic peaks of Hb (curve a) and Hb/TiO_2-CNT-CNF mixture (curve b) appeared at 407 nm with no peak shifting, indicating Hb in TiO_2-CNT-CNF composite maintained its complete structure.

FT-IR spectra can be applied to investigate the secondary structure of Hb and Hb/TiO_2-CNT-CNF. In Fig.2B the spectra for Hb and Hb/TiO_2-CNT-CNF mixture showed similar shape and position, especially amide I bonds at 1700-1600 cm^{-1} (C=O stretching vibrations of the peptide bonds) and amide II at 1600-1500 cm^{-1} (C-N stretching vibrations in combination with N-H bending). These results indicated the natural biological structure of Hb unchanged after interacted within TiO_2-CNT-CNF composite [26].

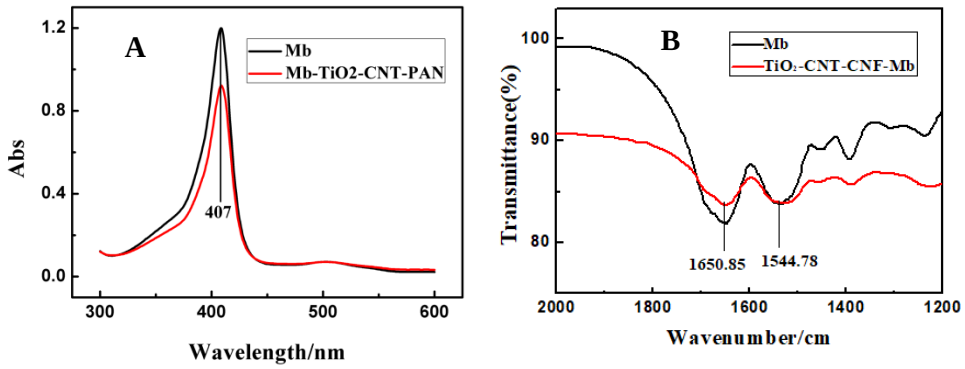

Figure 2. (A) UV-visible spectrum of (a) Hb in water, (b) Hb/TiO_2-CNT-CNF mixture; (B) FT-IR spectrum of (a) Hb, (b) Hb/TiO_2-CNT-CNF mixture.

3.3. Cyclic voltammograms of different electrodes

Voltammetric characteristics of various electrodes in O_2 free PBS (pH=5.0) were recorded and shown in Fig.3. Cyclic voltammetric curves of CILE (curve a), Nafion/CILE (curve b) and Nafion/TiO_2-CNT-CNF/CILE (curve c) gave stable background response. Couple of asymmetric redox peaks could be found on Nafion/Hb/CILE (curve d) and Nafion/Hb-TiO_2-CNT-CNF/CILE (curve e), which was corresponded to the typical electron transfer from hemin-active site in Hb to electrode surface. Compared with that of Nafion/Hb/CILE, Nafion/Hb/TiO_2-CNT-CNF/CILE exhibited larger redox faraday responses, which could be attributed to the presence of TiO_2-CNT-CNF nanocomposite contact with Hb on the modified electrode that provided a biocompatible and conductive interface to accelerate efficient electron transfer of Hb with CILE. It has been reported that nano metal oxide can improve the redox activity of iron proteins on the electrode surface [27-29]. TiO_2 nanoparticles can produce active small molecules on the surface, whcih have special catalytic and promotion activity to Hb [30]. These active small molecules may show certain impact on the protein framework as well as the heme rings with the enhancement of electrochemical activity of Hb [31]. However, when use nano metallic oxide alone, it is often to lose from the electrode surface with lower conductivity. Therefore, the immobilization of metal oxides with conductive supports is a valuable attempt. Synergistic effects of TiO_2 NPs with carbon nanomaterials can greatly increase the electrons diffusion length with enhanced catalytic activity to Hb [32].

Detailed electrode reaction processes were revealed by cyclic voltammetry and shown in Fig.4A. The redox peak currents were proportional to scan rate from 50 to 950 $mV{\cdot}s^{-1}$, and there also existed a linear relationships of redox peak potential (*Ep*) and *lnv* (Fig.4C). This phenomenon indicated a surface-controlled reaction process and the Laviron's equation are used to calculate the electrochemical parameters [33].

$$E_{pa} = E^{\circ\prime} + \frac{RT}{(1-\alpha)nF} lnv \quad (1)$$

$$E_{pc} = E^{\circ\prime} - \frac{RT}{\alpha nF} lnv \quad (2)$$

$$logk_s = \alpha\, log(1-\alpha) + (1-\alpha) log\alpha - log\frac{RT}{nFv} - (1-\alpha)\alpha\frac{nF\Delta E_p}{2.3RT} \quad (3)$$

Where α is the electron transfer coefficient, n is the electron transfer number, k_s is the standard electron transfer rate constant, v is the scan rate, ΔEp is the peak-to-peak separation. The solution of equation (3) can be solved using the data of scan rates. Based on these equations, n, α and k_s were obtained to be 1.05, 0.45 and 1.68 s^{-1}. Therefore there was one electron transfer on the electrode surface with the equation as Hb heme Fe(III)+ e → Hb heme Fe(II). Also the k_s value was bigger than reported value on titanate nanotubes modified electrode (k_s=0.85 s^{-1}) [34], proved a fast electron transfer rate due to carbon composite used.

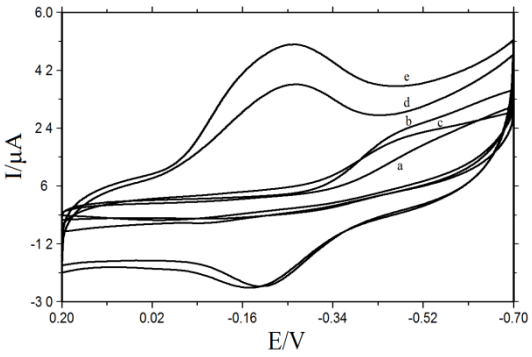

Figure 3. Cyclic voltammograms of (a) CILE, (b) Nafion/CILE, (c) Nafion/TiO_2-CNT-CNF/CILE, (d) Nafion/Hb/CILE, and (e) Nafion/Hb/TiO_2-CNT-CNF/CILE in 0.1 mol L^{-1} pH5.0 PBS at scan rate of 100 mV s^{-1}.

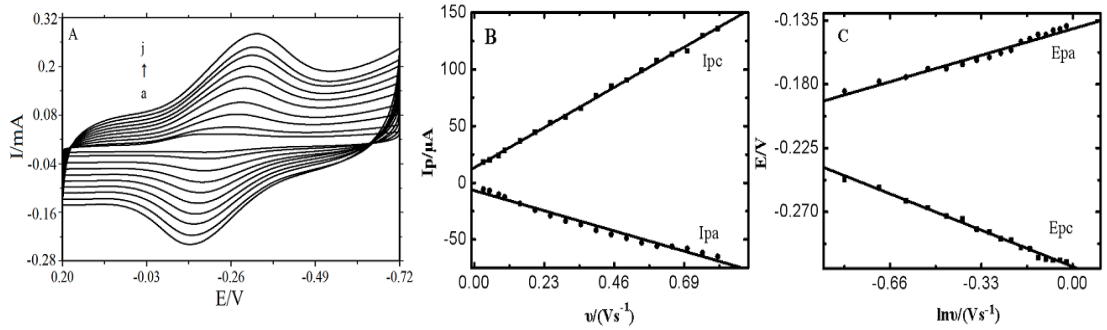

Figure 4. (A) Cyclic voltammograms of Nafion/Hb/TiO_2-CNT-CNF/CILE at different scan rates (curves a to j: 50, 100, 200, 300, 400, 500, 600, 700, 800, 900 mV·s^{-1}) in pH 5.0 PBS; (B) the relationship of Ipa and Ipc *vs.* scan rates (υ); (C) the relationship of Epa and Epc *vs.* lnυ.

The effect of pH value of PBS on voltammetric behaviors of Nafion/Hb/TiO_2-CNT-CNF/CILE was investigated from 3.0 to 7.0 with results shown in Fig. 5A. The maximum current of redox peak was observed in pH 5.0 PBS, indicating the highest direct electron transfer efficiency of Hb under this pH condition. The formal standard potential ($E^{0'}$) decreased linearly as a function of pH by a linear equation of $E^{0'}(mV)=-31.5pH-61.5(\gamma=0.999)$. The absolute slope of the linear equation (31.5 mV pH^{-1}) was smaller compared to the theoretical value (59 mV pH^{-1}), which may be due to the protonation effect around the electrochemical active center [35,36].

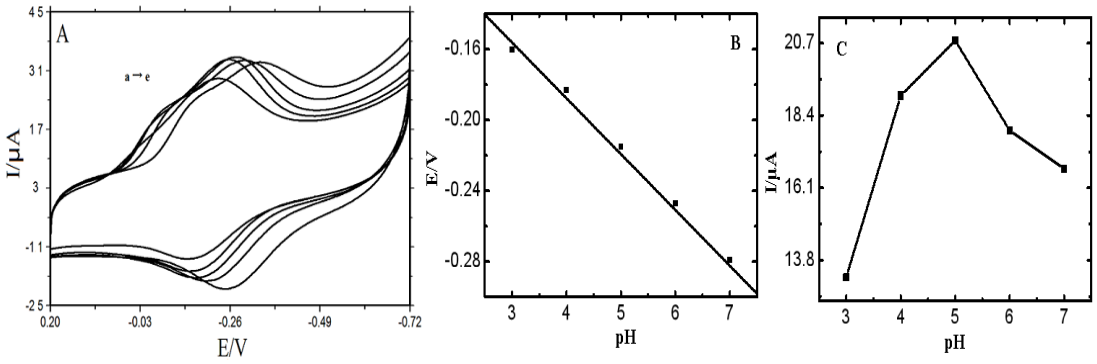

Figure 5. (A) Cyclic voltammograms of Nafion/Hb/TiO_2-CNT-CNF/CILE at different pH buffer (curves a to e: pH 3.0, 4.0, 5.0, 6.0,7.0); (B) the linear relationship of $E^{0'}$ *vs.* pH at scan rate of 0.1V s^{-1}; (C) the relationship between cathodic peak current and pH.

3.4. Electrocatalytic properties

Nafion/Hb/TiO_2-CNT-CNF/CILE had good catalytic properties toward the electro-reduction of TCA. With the increase of TCA content in pH 5.0 PBS, it was found that the reduction peak appeared near -0.288 V with the oxidation peak of Hb decreased to disappear gradually (Fig. 6A). When the content of TCA continued to increase, the second reduction peak was found at -0.474 V, indicating a two steps reduction electrocatalytic mechanism of TCA [37,38]. The new reduction peak current was linearly to TCA concentration from 5.0 mmol L^{-1} to 80.0 mmol L^{-1} with a regression equation of *Iss (μA) = 3.37C (mmol L^{-1}) +38.17 (γ = 0.997)* and the detection limit of 1.67 mmol L^{-1} (*3σ*). And when the concentration of TCA was exceeded 80.0 mmol L^{-1}, the current value approached to a fixed data, indicating a typical reaction of Michaelis-Menten dynamic mechanism. K_M^{app} is an important physical quantity of enzymatic catalytic reaction in investigating the reaction rate between enzymes and substrates. According to the Lineweaver-Burk equation [39], the K_M^{app} value of this catalytic reaction was deduced as 62.39 mmol L^{-1}, which was smaller than reported value such as 112.10 mmol L^{-1} [34] , meaning high activity for the reaction. A systematic comparison of this Hb electrochemical sensor with other reported references to TCA detection were summarized in table 1, which gave a relative wide linear range with low detection limit enough for route analysis.

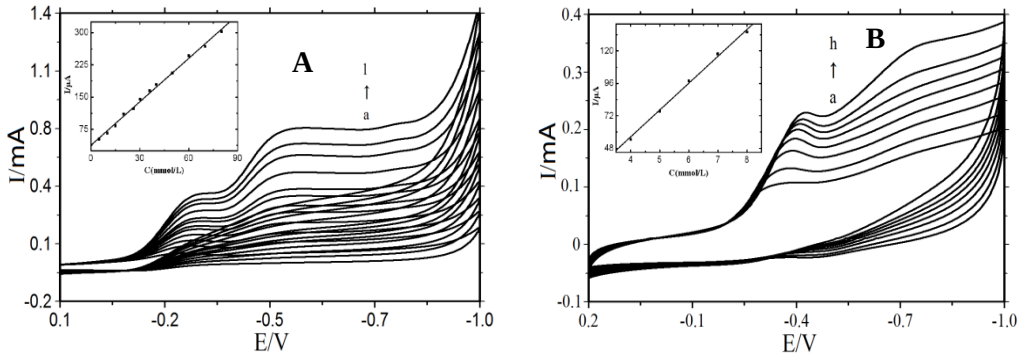

Figure 6. Cyclic voltammograms of Nafion/Hb/TiO_2-CNT-CNF/CILE in pH 5.0 PBS (A) with TCA (curves a to l: 5.0, 10.0, 15.0, 20.0, 26.0, 30.0, 36.0, 40.0, 50.0, 60.0, 70.0, 80.0 mmol L^{-1}), inset is the linear relationship of peak currents *vs.* TCA concentration; (B) with H_2O_2 (curves a to h: 4.0, 5.0, 6.0, 7.0, 8.0, 9.0,10.0, 12.0 mmol L^{-1}), inset is the linear relationship of peak currents *vs.* H_2O_2 concentration.

Table 1. Comparison of different Hb modified electrodes for TCA detection

Modifier	Linear range	Detection limit	Reference
Nano-diamond	1.1~30.0 mmol·L^{-1}	0.37 mmol·L^{-1}	[13]
Chitosan/Fe_3O_4 nanocomposite	5.70~205 μmol·L^{-1}	1.9 μmol·L^{-1}	[40]
Black phosphorene and PEDOT:PSS	3.0~460.0 mmol·L^{-1}	1.0 mmol·L^{-1}	[41]
g-C_3N_4 nanoparticle decorated 3D graphene-LDH network	0.2~36.0 mmol·L^{-1}	0.05 mmol·L^{-1}	[42]
Magnetic molecularly imprinted nanoparticles	1.0~160 mg·L^{-1}	0.25 mg·L^{-1}	[43]
Layered double hydroxides modified with amino functionalized ionic liquid	0.8~430 mmol·L^{-1}	0.194 mmol·L^{-1}	[44]
Graphene–copper sulfide nanocomposite	3.0~64.0 mmol·L^{-1}	0.20 mmol·L^{-1}	[45]
Titanium dioxide and carbon nanotube incorporated carbon nanofiber	5.0~80.0 mmol·L^{-1}	1.67 mmol·L^{-1}	This work

Nafion/Hb/TiO_2-CNT-CNF/CILE exhibited better electrocatalysis to the H_2O_2 reduction with curves shown in Fig. 6B. After adding H_2O_2 to PBS (0.1 mol L^{-1}, pH 5.0), a new reduction peak was found at -0.406V, indication that the H_2O_2 was reduced to water under the catalysis of Hb. With the increase of H_2O_2 content between 4.0 to 12.0 mmol L^{-1} in buffer, the reduction peak current increased with the linear fitting equation of $Iss(mA) = 19.85C(mmol\ L^{-1}) - 22.9 (\gamma = 0.987)$ and the detection limit as 1.00 mmol L^{-1} (3σ).

3.5. Sample detection

A drug sample (medical facial peel solution) that contained TCA (Shanghai Ika Biotechnology Co., China) was analyzed by use of Nafion/Hb/TiO_2-CNT-CNF/CILE, which diluted for 100 times by PBS and analyzed by the recommended procedure. As shown in table 2, the data and recovery were obtained by calibration curve method and standard addition method, respectively. Recovery was from 97.9% to 106.1%, showed that the modified electrode was suitable for the analysis of TCA content in medical facial peel solution.

Table 2. TCA analysis results in medical samples (n=3)

Sample	Detected (mmol L^{-1})	Added (mmol L^{-1})	Total (mmol L^{-1})	Recovery (%)
medical peeling solution	50.69	10.00	60.48	97.9
		20.00	71.56	105.3
		30.00	82.52	106.1

4. CONCLUSION

In this paper TiO_2-CNT-CNF nanocomposite was prepared by electrospinning and high temperature carbonization, which was modified on CILE surface to construct an electrochemical sensing platform. Furthermore, Hb and Nafion film were uniformly coated on the electrode surface to prepare an electrochemical Hb biosensor (Nafion/Hb/TiO_2-CNT-CNF/CILE), which was used to realize a fast direct electron transfer of Hb on the electrode. The network of high conductive CNF on CILE increased the contact with Hb, and the presence of TiO_2 NPs was benefit for the interaction with Hb molecules due to the presence of oxygenal group. This sensor was applied to the detection of TCA content in the medical facial peel solution with good experimental results, which showed the potential applications.

ACKNOWLEDGEMENTS
This work was financially supported by Open Foundation of Key Laboratory of Water Pollution Treatment and Resource Reuse of Hainan Province (2019-003).

References

1. M. Baghayeri, E. N. Zare, M. M. Lakouraj, *Microchim. Acta*, 182 (2015) 771
2. A. Sagasti, N. Bouropoulos, D. Kouzoudis, A. Panagiotopoulos, E. Topoglidis, J. Gutiérrez, *Materi als*, 10 (2017) 849
3. A. Panagiotopoulos, A. Gkouma, A. Vassi, C.J. Johnson, E. Topoglidis, *Electroanalysis*, 30 (2018) 1956
4. D. Q. Qian, W. B. Li, F. T. Chen, Y. Huang, N. Bao, H. Y. Gu, C. M. Yu, *Microchim. Acta*, 184 (201 7) 1977
5. Y. Ma, Y. M. Yu, M. Xu, X.F. Yan, D. C. Chen, M. Ma, *Nanosci. Nanotechnol. Lett.*, 8 (2016) 592
6. A. Maryam, R.E. Kenari, R. Farahmandfar, K. Abnous, S.M. Taghdisi, *Food Chem.*, 271 (2019) 54
7. J. Tom, H. A. Andreas, *Carbon*, 112 (2016) 230
8. Y. Y. Niu, R. Y. Zou, H.A. Yones, X. B. Li, X. Y. Li, X. L. Niu, Y. Chen, P. Li, W. Sun, *J. Chin. Chem. Soc.*, 65 (2018) 1127
9. G. L. Luo, Y. Deng, H. Xie, J. Liu, Si Mi, B. H. Li, G. J. Li, W. Sun, *Int. J. Electrochem. Sci.*, 14 (2 019) 2732
10. Y. Y. Niu, J. Liu, W. Chen, C. X. Yin, W. J. Weng, X. Y. Li, X. L. Wang, G. J. Li, W. Sun, *Anal. Met hods*, 44 (2018) 5297
11. Y. Zeng, H. H. Zhang, X. Wu, Y. Ke, P. P. Qu, Z. Zhu, *Anal. Methods*, 7 (2015) 6647
12. C. L. Fu, W. S. Yang, X. Chen, D. G. Evans, *Electrochem. Commun.*, 11 (2009) 997
13. H. Xie, X. Y. Li, G. L. Luo, Y. Y. Niu, R. Y. Zou, C. X. Yin, S. M . Huang, W. Sun, G. J. Li, *Diamo nd Relat. Mater.*, 97 (2019) 107453
14. Z. Sadat, A. Mohsen, Mohsennia, H. Rafiee-Pour, *J. Solid State Electrochem.*, 23 (2019) 2233
15. J. X. Li, L. H. Zhou, X. Han, J. Hu, H. L. Liu, J. Xu, *Sens. Actuators, B*, 138 (2009) 45
16. S. Palanisamy, Y. Wang, S. Chen, *Microchim. Acta*, 183 (2016) 1953
17. W. Sun, X. Q. Li, Z.Q. Zhai, K. Jiao, *Electroanalysis*, 20 (2008) 2649
18. Y. Y. Niu, X. Q. Li, H. Xie, G. Luo, R. Y. Zou, Y. Xi, G. Li, W. Sun, *J. Chin. Chem. Soc.*, (2019) 1
19. X. Chen, H. Yan, Z. Shi, Y. Feng, J. Li, Q. Lin, X. Wang, W. Sun, *Polym. Bull.*, 74 (2017) 75
20. J. Liu, W. Weng, H. Xie, G. Luo, G. J. Li, W. Sun, *ACS Omega*, 4 (2019) 15653
21. C. M. Yang, B.H. Kim, *J. Alloys Compd.*, 749 (2018) 441
22. T. Meng, J. C. Gao, Y. Liu, J. H. Zhu, H. Zhang, L. Ma, M. Xu, C. Li, J. Jiang, *ACS Appl. Mater. In*

terfaces, 11 (2019) 26798
23. Z. Wang, C. Liu, G. F. Shi, H. Ma, X. Jiang, Q. Zhang, H. Zhang, Y. Su, J. Yu, *Ionics*, 25 (2019) 50 35
24. Y. Y. Niu, H. Xie, G. L. Luo, W. J. Weng, C. X. Ruan, G. J. Li, W. Sun, *RSC Adv.*, 9 (2019) 4480
25. Y. Y. Niu, J. Liu, W. Chen, C. X. Yin, W. J. Weng, X. Li, X. Y. Wang, G.J. Li, W.Sun, *Anal. Method s*, 10 (2018) 5297
26. H. Y. Yang, S.N. Yang, J. L. Kong, A.C. Dong, S.N. Yu, *Nat. Protoc.*, 10 (2015) 382
27. F. Shi, W. C. Wang, S. X. Gong, B. X. Lei, G. J. Li, X. M. Lin, Z. F. Sun, W. Sun, *J. Chin. Chem. S oc.*, 62 (2015) 554
28. Z. H. Zhu, L. N. Qu, Q. J Niu, Y. Zeng, W. Sun, X.T. Huang, *Biosens. Bioelectron.*,26 (2010) 2119
29. A. Sagasti, N. Bouropoulos, D. Kouzoudis, A. Panagiotopoulos, E. Topoglidis, J. Gutiérrez, *Materi als*, 10 (2017) 849
30. H. Al-Ekabl, N. Serpone, *J. Phys. Chem.*, 92 (1988) 5726
31. H. Zhou, X. Gan, J. Wang, X. L. Zhu, G. X. Li, *Anal. Chem.*, 77 (2005) 6102
32. J. G. Yu, J. J. Fan, B. Cheng, *J. Power Sources*, 196 (2011) 7891.
33. E. Laviron, *J. Electroanal. Chem.*, 101 (1979) 19
34. W. J. Weng, J. Liu, C. X. Yin, H. Xie, G. L. Luo, W. Sun, Guangjiu Li, *Int. J. Electrochem. Sci.*, 14 (2019) 4309
35. A. M. Bond, Modern polarographic methods in analytical chemistry, Marcel Dekker, (1980) New Y ork, U.S.A.
36. L Meites, Polarographic techniques, Wiley, (1965) New York, U.S.A.
37. J. F. Rusling, *Chem. Inf.*, 31 (1998) 363
38. W. Sun, F. Hou, S. X. Gong, L. Han, W. C. Wang, F. Shi, J. W. Xi, X. L. Wang, G. J. Li, *Sens. Actu ators, B*, 219 (2015) 331
39. R. A. Kamin, G. S. Wilson, *Anal. Chem.*, 52 (1980) 1198
40. H. Wang, C. M. Yu, H. Y. Gu, Y. F. Tu, *J. Solid State Electrochem.*, 20 (2016) 1337
41. X. Y. Li, X. L. Niu, W. S. Zhao, W. Chen, C. X. Yin, Y. L. Men, G. J. Li, W. Sun, *Electrochem. Co mmun.*, 86 (2018) 68
42. T. R. Zhan, Z. W. Tan, X. J. Wang, W. G. Hou, *Sens. Actuators, B*, 255 (2018) 149
43. Y. Yuan, J. X. Wang, X. J. Ni, Y. H. Cao, *J. Electroanal. Chem.*, 834 (2019) 233
44. T. R. Zhan, X. J. Wang, Y. M. Zhang, Y. Song, X. L. Liu, J. Xu, W. G. Hou, *Sens. Actuators, B* 220 (2015) 1232
45. F. Shi, W. Z. Zheng, W. C. Wang, F. Hou, B. X. Lei, Z. F. Sun, W. Sun, *Biosens. Bioelectron.*, 64 (2 015) 131